THE JOURNAL OF BIOLOGICAL CHEMISTRY VOL. 285, NO. 32, pp. 24432–24438, August 6, 2010

The Sodium Bicarbonate Cotransporter (NBCe1) Is Essential for Normal Development of Mouse Dentition*

Received for publication, February 17, 2010, and in revised form, April 27, 2010 Published, JBC Papers in Press, June 6, 2010, DOI 10.1074/jbc.M110.115188

Rodrigo S. Lacruz[‡], Antonio Nanci[§], Shane N. White[¶], Xin Wen[‡], HongJun Wang[‡], Sylvia F. Zalzal[§], Vivian Q. Luong[¶], Verna L. Schuetter[¶], Peter S. Conti[‖], Ira Kurtz[**], and Michael L. Paine[‡1]

*From the [‡]School of Dentistry, Center for Craniofacial Molecular Biology, University of Southern California, Los Angeles, California 90033, the [§]Faculty of Dentistry, Laboratory for the Study of Calcified Tissues and Biomaterials, Université de Montréal, Montréal, Quebec H3C 3J7, Canada, the [¶]School of Dentistry, UCLA, Los Angeles, California 90095-1668, the [‖]Department of Radiology, Molecular Imaging Center, University of California Keck School of Medicine, Los Angeles, California 90033, and the **David Geffen School of Medicine at UCLA, Los Angeles, California 90095*

Proximal renal tubular acidosis (pRTA) is a syndrome caused by abnormal proximal tubule reabsorption of bicarbonate resulting in metabolic acidosis. Patients with mutations to the *SLC4A4* gene (coding for the sodium bicarbonate cotransporter NBCe1), have pRTA, growth delay, ocular defects, and enamel abnormalities. In an earlier report, we provided the first evidence that enamel cells, the ameloblasts, express NBCe1 in a polarized fashion, thereby contributing to trans-cellular bicarbonate transport. To determine whether NBCe1 plays a critical role in enamel development, we studied the expression of NBCe1 at various stages of enamel formation in wild-type mice and characterized the biophysical properties of enamel in NBCe1$^{-/-}$ animals. The enamel of NBCe1$^{-/-}$ animals was extremely hypomineralized and weak with an abnormal prismatic architecture. The expression profile of amelogenin, a known enamel-specific gene, was not altered in NBCe1$^{-/-}$ animals. Our results show for the first time that NBCe1 expression is required for the development of normal enamel. This study provides a mechanistic model to account for enamel abnormalities in certain patients with pRTA.

Enamel development can be subdivided into three major functional stages: presecretion, secretion, and maturation (1). Crystal nucleation and growth involve the release of hydrogen ions, which results in a decrease of the local pH to very acidic levels and could lead to demineralization of the crystals (2). Mineral deposition in amelogenesis requires tight control of pH via specific H^+/base transport processes. The SLC4 family of bicarbonate transport proteins plays an important role in regulating intra- and extracellular pH and are arguably considered the most important buffer system in eukaryotic cells (3). Two members of the SLC4 (solute carrier bicarbonate transport family) have been identified in ameloblasts (4, 5). The *SLC4A2* and *SLC4A4* genes encode the anion exchanger (AE2)[2] and the electrogenic bicarbonate cotransporter (NBCe1), respectively (3). Paine *et al.* (2008) investigated the expression of AE2 and NBCe1 in ameloblasts by immunohistochemistry and reverse transcribed-PCR (RT-PCR) (5). AE2 was expressed apically, whereas NBCe1 was expressed on the basolateral membrane (5). Additional RT-PCR experiments showed that ameloblasts express the AE2a and NBCe1-B variants.

Mice with a targeted disruption to the *Slc4a4* gene locus (NBCe1$^{-/-}$ mice) have a severe and fatal phenotype (6). They exhibited severe metabolic acidosis, growth retardation, reduced plasma Na^+, hyperaldosteronism, splenomegaly, intestinal obstructions, and die before weaning (6). NBCe1$^{-/-}$ mice also are described as having an abnormal dentition with "chalk-white" and "brittle" enamel that is easily fractured (6). Patients with NBCe1-A loss of function mutations also have a tooth phenotype (7, 8). For example, Inatomi *et al.* (8) describe the enamel defect seen in one affected individual as "raised, rough, and white chalk-like."

Based on this evidence, Paine *et al.* (5, 9) hypothesized that NBCe1 plays an important role in trans-cellular bicarbonate secretion during amelogenesis. However, there is no information regarding the requirement of NBCe1 in tooth and enamel formation in part because extensive analysis of the dentition of patients with NBCe1 mutations is lacking. In the present study, ameloblasts cells dissected from the late secretory stage of amelogenesis were analyzed to investigate our hypothesis that NBCe1 plays an important role in tooth formation. NBCe1$^{-/-}$ and wild-type mice were used as a model system. Our results demonstrate for the first time that enamel development in mammals requires NBCe1 and more specifically the NBCe1-B variant.

EXPERIMENTAL PROCEDURES

Animals and Animal Husbandry—All vertebrate animal manipulation complied with institutional and federal guidelines. NBCe1$^{+/-}$ mice were a kind gift from Dr. Gary Shull (6). The genotypes of the offspring were established using DNA from tail biopsy, and primers and RT-PCR conditions were done as published previously (6). Litters from heterozygous parents typically produced 6–10 animals, and offspring numbers followed mendelian genetics, with ~25% wild-type, 50% NBCe1$^{+/-}$, and 25% NBCe1$^{-/-}$ pups available from each litter for studies, which meant all imaging and mechanical testing could be done using animals from the same litter. All specimens

* This work was supported, in whole or in part, by National Institutes of Health Grants DE013404 and DE019629 (to M. L. P.), DK058563 and DK077162 (to I. K.), and S10RR019253 (to P. S. C.). This work was also supported by the Canadian Institutes of Health Research (to A. N.).

[1] To whom correspondence should be addressed. Tel.: 323-442-1728; Fax: 323-442-2981; E-mail paine@usc.edu.

[2] The abbreviations used are: AE, anion exchanger; pRTA, proximal renal tubular acidosis; Cftr, cystic fibrosis trans-membrane conductance regulator; SEM, scanning electron microscopy; RT, reverse transcribed.

for study were sacrificed at between 12–14 days post-natal. This is the time at which the life expectancy of NBCe1$^{-/-}$ animals declines drastically (6). NBCe1$^{-/-}$animals received the same diet and were kept under the same conditions, requiring no special attention up to the time they were sacrificed.

Tissue Dissection and RT-PCR—Ameloblasts from the late secretory stage of 7-day-old mice were dissected from mandibular incisors following protocols described previously (10, 11). Reverse transcription reactions were performed using the Bio-Rad iScript^{TM} cDNA synthesis kit (random hexamer primers; Bio-Rad) following the manufacturer's suggested protocols. PCR reactions were performed using a Titanium^{TM} TaqDNA polymerase kit (Clontech, Mountain View, CA). Gene-specific primers have been described previously for AE2a, NBCe1-A, NBCe1-B, NBCe1-C, and β-actin (5), and the primers used for mouse cystic fibrosis trans-membrane conductance regulator protein (Cftr) were forward (5′-TGTTACACTCCATTCT-TCACGCCCCTATGTC-3′) and reverse (5′-TCCTGCCT-TCAGATTCCAGTTGTTTGAGC-3′) to give a product of 291 bp. A mouse kidney was dissected from a 4-week-old Swiss Webster male mouse and processed immediately for total RNA isolation using the Qiagen RNase mini kit and DNase. PCR reactions were set as follows: 94 °C initial denaturation (4 min); then 94 °C (1 min), 65 °C (1 min), 72 °C (1 min) ($\times$ 35 cycles); 72 °C (5 min, final extension), followed by a return to room temperature.

Micro-CT Analysis—Mandibles of 12-day-old NBCe1$^{-/-}$ mice were dissected, dehydrated, and preserved in 70% alcohol. The samples were analyzed with Siemens MicroCAT® II at the University of Southern California Molecular Imaging Center. The MicroCAT images were acquired with the x-ray source at 80 kVp and 250 μA. The data were collected at a high resolution of 10 μm. The reconstruction was done with COBRA, and the voxel size was 10 μm. The acquisition proceeded for 28–29 min (550 rotation steps, 210° rotation). For each sample, 1024 $\times$ 1024 slices were taken to cover the entire mandible.

Staining of Incisor with pH Indicator—Animals were sacrificed at day 12 post-natal, as at this age, life expectancy dramatically decreases in NBCe1$^{-/-}$ animals. Mandibles of wild-type and NBCe1$^{-/-}$ mice were immediately dissected and placed in liquid nitrogen for 24 h and subsequently placed in a lyophilizer overnight. Incisors were then dissected out of the bone, the enamel organ was removed by gentle wiping with a moist gauze in the incisal direction, and the specimens were then placed in either methyl red or Fisher's pH universal indicator.

Immunoperoxidase Immunohistochemistry—In our previous report, we incorrectly stated that the tissues used for anti-NBCe1 immunohistochemistry were formalin-fixed. Rather, tissues were fixed in Carnoy's solution, and Carnoy's was the fixative used again in this study. The anti-NBCe1 primary antibody has been described previously (5, 12) and was used at a 1:100 dilution for immunoperoxidase using the Zymed Laboratories, Inc. Histomouse AEC kit as per the manufacturer's instructions.

Immunofluorescence Immunohistochemistry—Samples were fixed and decalcified with 2% paraformaldehyde and 5% EDTA, treated with sucrose buffer ($\times$2) embedded with optical coherence tomography compound (TissueTek® O.C.T.^{TM} Compound; Sakura Finetek USA, Inc., Torrence, CA), and frozen for cryosectioning prior to immunofluorescence. The anti-NBCe1 primary antibody (5, 12) was used at a 1:100 dilution. The secondary antibody used was Texas Red-conjugated goat anti-rabbit antibody (Molecular Probes, Invitrogen).

Western Blot—First and second molars from the right and left mandibles were dissected from 3–4-day-old pups using a standard dissecting stereoscopic microscope. Samples were lysed in 2$\times$ SDS-PAGE loading buffer (50 μl per mouse) using a tissue homogenizer and vortexing. The samples were boiled for 5 min, chilled on ice, and centrifuged to remove residual debris. The protein lysate was resolved to size on a 12% SDS-PAGE (10 μl each), and a Western blot was performed using the Amersham Biosciences ECL kit (GE Healthcare). Antibodies to mouse amelogenin and glyceraldehyde-3-phosphate dehydrogenase had been previously described in Ref. 13 and used at a dilution of 1:1,000 and 1:2,000 respectively.

Scanning Electron Microscopy (SEM)—For SEM analyses, the heads of mice from the various experimental group ages (12–14-day-old) were fixed by immersion in 4% paraformaldehyde overnight and then placed in phosphate-buffered saline. The right and left side of the lower mandibles, or hemimandibles, were isolated and soft tissues were cleaned off. Some incisors were dissected out under a microscope, subsequently air dried, and fractured at the same level ~3–4 mm below the tip. Specimens were sputter-coated with gold palladium to be examined under SEM. Some hemimandibles were dehydrated in graded concentrations of acetone and embedded in epoxy resin, others were examined in the wet state in a JEOL 6460LV variable pressure scanning electron microscope operated at 20 kv with a pressure of 50–70 pascals. Cross-cut slices were made though the embedded hemimandibles. One surface of the slices was polished, and the slices were then examined under similar conditions in the JEOL 6460LV. At low vacuum, the instrument uses a backscattered electron detector for imaging. Images from slices obtained from similar regions were compared. Some polished samples were coated with carbon in a Baltec MED 020 coating system (Balzers AG) and examined using the backscattered electron detector in a JEOL 7400F field emission scanning electron microscope operated at 20 kV.

Microindentation—Microindentation techniques were used to measure enamel and dentin hardness (14–17). For all mechanical testing, 12-day-old animals were studied. Thirteen freshly extracted intact murine lower left incisor teeth, from two litters containing three wild-type, seven heterozygotic, and three homozygotic mice were studied. Teeth were kept moist at all times, mounted in slow-set epoxy resin, and sequentially ground in the sagittal plane to a 0.1 μm alumina finish using a semiautomatic polisher (Buehler, Lake Bluff, IL). Loads of up to 50 g were used with dwell times of 20 s using a customized manually operated Vickers microhardness tester. For each tooth, 15 indentations were made on enamel, and 15 indentations were made on dentin, with the means being used to describe each tooth. All indentations were made on the erupted incisal thirds of the teeth, but not including the incisal-most 1 mm. The indentations were made toward the center of the enamel and dentin layers, not

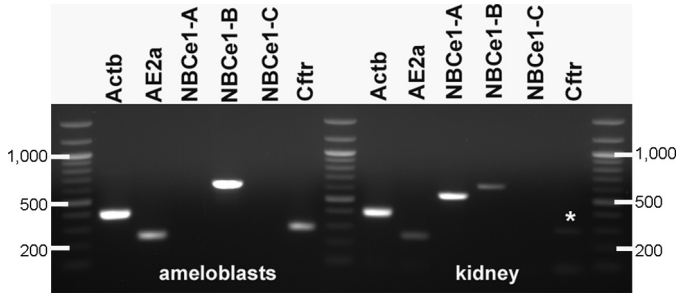

FIGURE 1. **Expression of NBCe1 variants in ameloblasts dissected from the late secretory stage of amelogenesis in 7-day-old mice and in kidney.** The only isoform expressed by ameloblast is NBCe1-B as reported previously in the ameloblast cell line LS8 (5). In kidney, NBCe1-A and NBCe1-B are expressed as reported in Brandes *et al.* (18). A faint but clear band is apparent for Cftr in kidney cells, identified by an *asterisk*. β-actin (*Actb*) is used here as a positive control, cDNA transcript. A DNA 100-bp ladder also is included 3× on the gel.

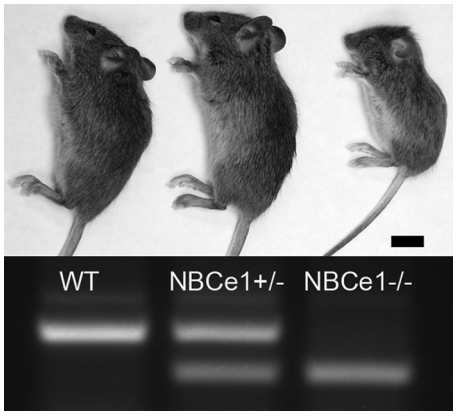

FIGURE 2. **Gross phenotype of NBCe1$^{-/-}$ mice at 10 days of age.** Wild-type (*far left*), NBCe1$^{+/-}$ (*center*), and NBCe1$^{-/-}$ (*far right*) littermates (*top panel*) were genotyped (*bottom panel*) by RT-PCR as described previously (6). The body length of NBCe1$^{-/-}$ mice is ~75% of the body length of both wild-type and NBCe1$^{+/-}$ mice. *Scale bar*, 1 cm.

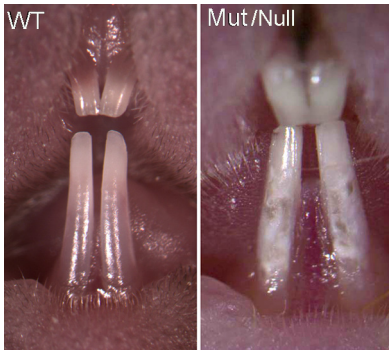

FIGURE 3. **Gross anatomy of upper and lower incisor teeth of NBCe1$^{-/-}$ mice at 14 days of age.** Wild-type animal (*WT*; *left panel*) is shown here with an NBCe1$^{-/-}$ (mutant or null, *Mut/Null*; *right panel*) littermate. NBCe1$^{-/-}$ animals show the chalky-white enamel of the incisor teeth. Magnification was increased to image the NBCe1$^{-/-}$ animal to show its abnormal enamel in more detail. The characteristic iron-induced pigmentation of mice incisors is absent in the enamel of NBCe1$^{-/-}$ animals.

on surface enamel or dentin. Indentations were examined by light microscopy, using polarization, interference, light/dark field, and trans-illumination techniques; measurements were made using a digital micrometer. Descriptive statistics, one-way analysis of variance ($p < 0.05$), and Tukey multiple comparisons testing ($p < 0.05$) were used to analyze the data.

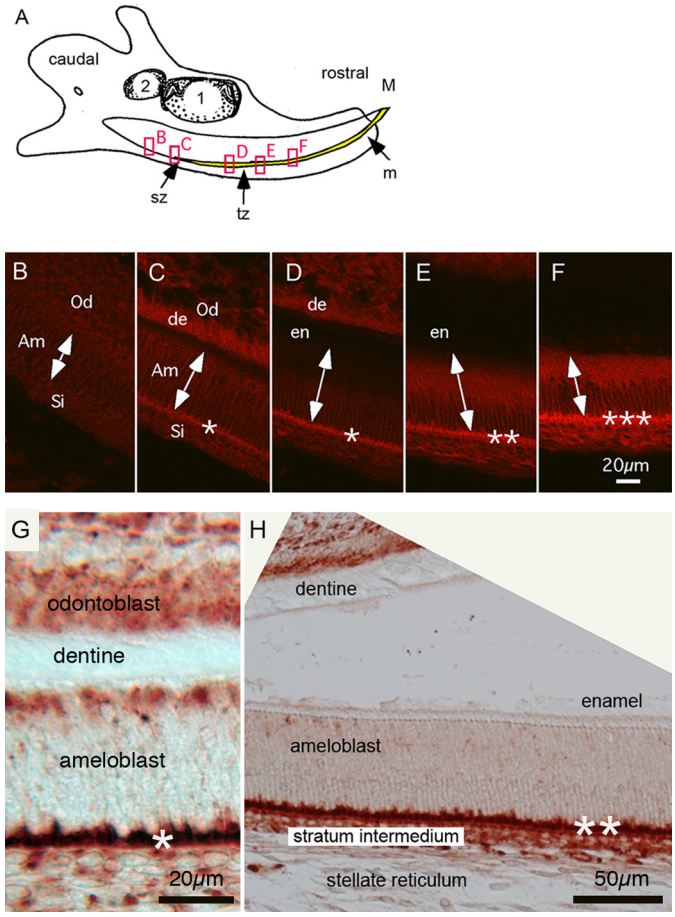

FIGURE 4. **Immunofluorescence (*IF*) and immunoperoxidase of NBCe1 in polarized ameloblast cells.** *A*, illustration of a sagittal view of a mandible of 3-day-old wild-type mouse. The mature (*M*) end and the caudal or growing end (*GE*) of the incisor tooth are identified. Also identified are the secretory zone (*sz*), transitional zone (*tz*; the zone between enamel matrix secretion and enamel maturation) and mature end (*m*) of the incisor enamel. *Boxed regions* from *left* to *right* are approximate regions shown in *B–F*. *B–F*, immunoflouresecence of NCBe1 in a 3-day-old developing mandibular incisor. Expression of NBCe1 is seen at the various stages of amelogenesis. *B*, nonpolarized presecretory stage. *C*, early stage secretory, signal is recognizable at this point. *D*, secretory stage showing clear expression of NBCe1 at basolateral pole. *E* and *F*, the highest expression of NBCe1 is found in the cells at the end of the secretory stage. *Double-headed arrows* identify orientation and basal (*lower*) and apical (*upper*) extremes of ameloblast cells. *Asterisks* identify relative levels of NBCe1 expression. *Am*, ameloblast; *Od*, odontoblast; *Si*, Stratum intermedium; *en*, enamel; and *de*, dentin. *G* and *H*, immunoperoxidase of polarized, early secretory (*G*) and secretory stage (*H*) ameloblasts of the mandibular incisor. Note that a separation artifact between the enamel and dentin occurred during tissue preparation from immunoperoxidase staining (*H*). *Scale bars*: *B–F*, 20 μm; *G*, 20.0 μm; and *H*, 50.0 μm.

RESULTS

RT-PCR—The expression of NBCe1 variants in ameloblasts and in kidney is shown in Fig. 1. Ameloblasts express only the NBCe1-B variant, whereas in kidney, both NBCe1-A and NBCe1-B are expressed as reported previously (18). The variant NBCe1-C only has been reported in brain tissue to date (19) and is not present in either ameloblast or kidney cells. These data confirm that NBCe1-B is the only isoform of NBCe1 expressed by ameloblast cells *in vivo*, as described previously from cultured ameloblast-like LS8 cells (5). From these data, we also can confirm that the AE2a isoform of AE2 is expressed, as well as Cftr, in ameloblast cells *in vivo* (Fig. 1).

Gross Phenotypical Analysis of Wild-type, NBCe1$^{+/-}$ and NBCe1$^{-/-}$ Mice—At 12–14 days of age, the NBCe1$^{-/-}$ mice were visibly smaller than their littermates, shorter in body length with a weight of ~30% less than wild-types or NBCe1$^{+/-}$ mice (Fig. 2), and showed abnormal locomotor behavior (6). The gross appearance and behavior of wild-type and NBCe1$^{+/-}$ animals were similar. NBCe1$^{-/-}$ mice were fully dentate, as observed during sectioning prior to imaging analysis, and also by micro-CT analysis of 12-day-old NBCe1$^{-/-}$ mice ($n = 3$) (data not shown). The incisor teeth of the wild-type and NBCe1$^{-/-}$ mice pictured in Fig. 2 were photographed at low power magnification (Fig. 3) to show the gross anatomical differences between these two animals. The enamel of the maxillary and mandibular incisor teeth of NBCe1$^{-/-}$ mice appeared hypoplastic (*i.e.* chalky-white and opaque), when compared with their wild-type littermates. No apparent differences were observed between the incisors of wild-type and NBCe1$^{+/-}$ mice (data not shown).

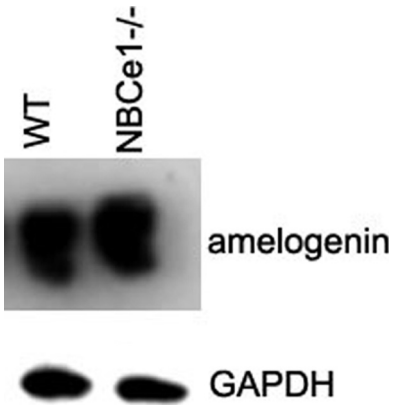

FIGURE 5. **Expression of amelogenin is not affected in NBCe1$^{-/-}$ animals at 3 days of age.** The expression of amelogenin in NBCe1$^{-/-}$ (mutant) mice is similar to the expression seen in NBCe1$^{+/+}$ (wild-type; *WT*) mice. Glyceraldehyde-3-phosphate dehydrogenase (*GAPDH*) protein levels served as a control.

Staining of Incisors—Bands of normal and acidic pH were observed on the labial surface of incisors of wild-type, as reported previously (20). Eight NBCe1$^{-/-}$ animals were used to analyze pH staining. However, the enamel of these animals was very soft and commonly detached from the underlying dentine during preparation of the specimens, either during dissection or during the removal of the enamel cell layer with a moist gauze. After preparation, the remaining enamel patches showed, in all cases, a different staining result when immersed in pH indicator solutions (data not shown).

Higher levels of NBCe1 Are Apparent During Late Secretory Stage of Amelogenesis—Using sagittal sections of 4-day-old wild-type mandibular incisors, immunofluorescent analysis showed that the expression of NBCe1 is negligible in ameloblasts in the presectetory stage of amelogenesis (Fig. 4*B*), increased steadily during the early secretory stage (Fig. 4, *C–E*), and reached a peak in expression level during the late secretory stage of amelogenesis (Fig. 4*F*). Additionally, using the same anti-NBCe1 antibody and immunoperoxidase labeling, labeling was seen to be limited to the basal pole of secretory ameloblasts (Fig. 4, *G* and *H*, identified by an *asterisk*). NBCe1 expression also is seen in the cells of the stratum intermedium, odontoblasts, and pulpal cells (Fig. 4*G*). Thus, as reported here and previously (5), NBCe1 expression is limited to the basolateral poles of polarized ameloblast cells with expression greatest in the late secretory zones (Fig. 4, *C–G*).

Western Blot Analyses—Amelogenin is the dominant secreted protein produced from ameloblast cells and comprises ~90% of the organic enamel matrix (21). Amelogenin expression levels were assessed in mutant animals to establish whether ameloblast secretory pathways were disrupted as a result of the NBCe1-null phenotype. Amelogenin and glyceraldehyde-3-phosphate dehydrogenase (control) expression in NBCe1$^{+/+}$, NBCe1$^{+/-}$, and NBCe1$^{-/-}$ littermates was examined by Western blot analysis in molars extracted from 3-day-old animals. Amelogenin expression is not affected in NBCe1$^{-/-}$ animals when compared with either NBCe1$^{+/-}$ or NBCe1$^{+/+}$ (Fig. 5).

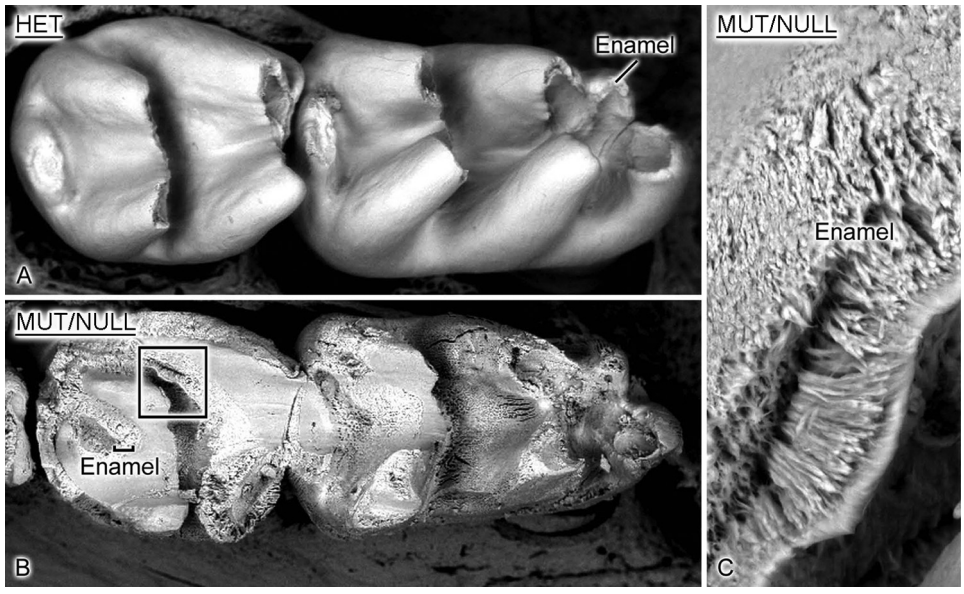

FIGURE 6. **SEM image of mandibular molars of NBCe1 mutant animals.** SEM image of molars of NBCe1$^{+/-}$ (*A*) and NBCe1$^{-/-}$ mice (*B*). NBCe1$^{-/-}$ molars show abnormal enamel phenotype, as also seen in the incisors. The specimens shown here were imaged directly under the SEM without sectioning. *C*, a higher power SEM image of the NBCe1$^{-/-}$ mice showing disrupted prismatic structure. *MUT/NULL*, mutant or null. *HET*, heterozygous.

SEM and Backscattered SEM—Fig. 6 shows details of the first and second mandibular molars of 12-day-old NBCe1$^{+/-}$ and NBCe1$^{-/-}$ littermates and demonstrates an abnormal molar enamel architecture with severe disruption of the enamel layer in the NBCe1$^{-/-}$ (mutant) mice (Fig. 6*B*) compared with the normal enamel phenotype of NBCe1$^{+/-}$ mice (*A*). Fig. 6*C* shows a higher power SEM image of the altered enamel microstructure of NBCe1$^{-/-}$ mice.

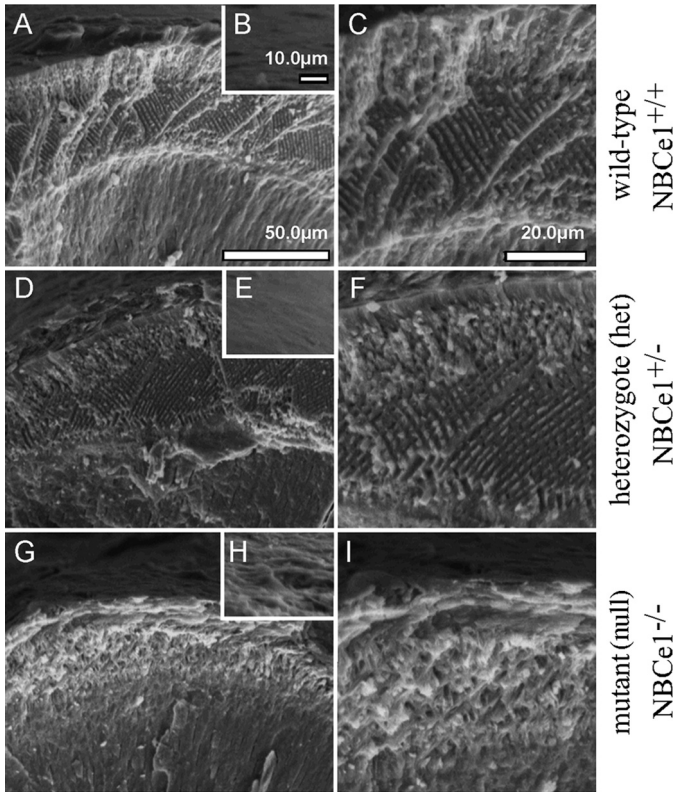

FIGURE 7. **SEM images of mature enamel cross-sections in NBCe1$^{-/-}$ mouse incisors.** This Fig. shows the mature enamel regions of wild-type (*A*, *B*, and *C*), NBCe1$^{+/-}$ (*D*, *E*, and *F*), and NBCe1$^{-/-}$ (*G*, *H*, and *I*). Incisors were dissected and air-dried and mechanically fractured perpendicular to the enamel surface at approximately the same anatomical region of the erupted crowns and then imaged by SEM. The dentin-enamel junction is clearly apparent in all teeth. Enamel thickness measurements from fractured surfaces does not provide accurate linear measurements; however, each of the NBCe1$^{-/-}$ mice showed less thickness than wild-type or NBCe1$^{+/-}$ littermates, which was confirmed by micro-CT analyses (data not shown). The prismatic enamel in a cross-section of wild-type and NBCe1$^{+/-}$ mice are very similar, and the same applies to the outer surface of the enamel. However, NBCe1$^{-/-}$ enamel architecture and outer enamel surface topography appears abnormal. *Scale bar*: *A*, *D*, and *G*, 50.0 μm; *B*, *E*, and *H*, 10.0 μm; and *C*, *F*, and *I*, 20.0 μm.

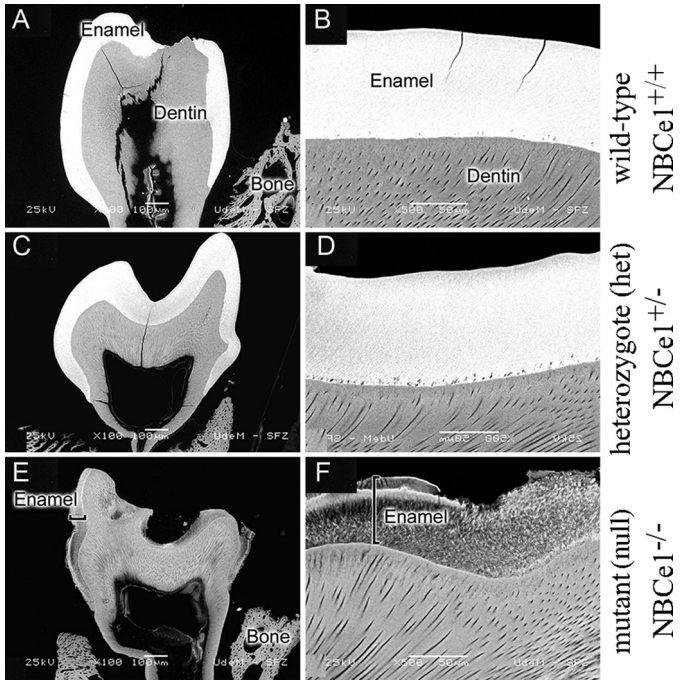

FIGURE 8. **Backscattered scanning electron microscope (SEM) imaging of NBCe1 mutant animals.** Backscattered SEM image of first mandibular molars of NBCe1$^{+/+}$ (*A* and *B*), NBCe1$^{+/-}$ (*C* and *D*), and NBCe1$^{-/-}$ animals (*E* and *F*) showing a significantly lower signal in the NBCe1$^{-/-}$ animals indicative of extremely poor mineralization of the enamel (*F*). *Scale bars* are shown in each *panel*.

The fractured surface of the incisors of wild-type, NBCe1$^{+/-}$, and NBCe1$^{-/-}$ mice are shown in Fig. 7 exposing its enamel microstructure under the low and high power SEM. Microstructural organization of the enamel in wild-type and NBCe1$^{+/-}$ mice appeared similar (Fig. 7, *A* and *C* compared with *D* and *F*); whereas the phenotype of NCBe1$^{-/-}$ animals is visibly abnormal (Fig. 7, *G* and *I*). Fig. 7 *insets B*, *E*, and *H* show the outer surface of enamel, which in NBCe1$^{-/-}$ animals (*inset H*) lacks the smooth appearance of NBCe1$^{+/+}$ (*inset B*) and NBCe1$^{+/-}$ (*inset E*) animals.

Figs. 8 and 9 show backscattered SEM images of the sectioned mandibular molars and incisors of NBCe1$^{+/+}$ (wild-type), NBCe1$^{+/-}$ (heterozygote), and NBCe1$^{-/-}$ (mutant) mice. Enamel from NBCe1$^{-/-}$ teeth (Fig. 8, *E* and *F*; Fig. 9, *C* and *D*) generated a lower backscattered electron contrast compared with NBCe1$^{+/+}$ or NBCe1$^{+/-}$ enamel (Fig. 8, *B* and *D*; Fig. 9, *A* and *B*), indicating that the enamel in mutant mice is hypomineralized. In incisors, whereas rods are readily apparent even in young enamel from NBCe1$^{+/+}$ and NBCe1$^{+/-}$ mice (Fig. 9, *A* and *B*), these are much less evident in NBCe1$^{-/-}$ mice, particularly in older enamel (Fig. 9, *C* and *D*).

It is important to note that the imaging done on the molar teeth for 12-day-old NBCe1$^{-/-}$ mice is at a time prior to the their eruption into the oral cavity, which occurs at ~day 16 for the first molar and day 18 for the second molar (22). Thus, the pH of the saliva in these mutant animals does not impact on the enamel architecture as seen in Figs. 6 and 8, but rather, the phenotypes observed in the SEM analyses described here, clearly are indicative of developmental disruptions occurred during enamel formation in the pre-eruptive phase, thus being unaffected by salivary pH.

Microindentation—The enamel of NBCe1$^{-/-}$ animals was not measurable, due to the extreme softness and fragility of the tissue; hence, this enamel was manifestly softer than wild-type or NBCe1$^{+/-}$ animals. No differences were found between wild-type and NBCe1$^{+/-}$ animals for enamel or dentin hardness (Table 1). Interestingly, our data on the dentin of NBCe1$^{-/-}$ animals is ~22% softer than wild-type and NBCe1$^{+/-}$ animals (Table 1) suggesting that dentinogenesis also may be influenced by the NBCe1 Na^+/HCO_3^- cotransporter function. This finding is not unreasonable considering that NBCe1 expression is apparent in odontoblast cells (Fig. 4, *G* and *H*).

DISCUSSION

One of the earliest reports of congenital renal and dental disease being present together is from Winsnes *et al.* (23). Winsnes and collaborators reported the cases of two brothers with severe hyperchloremic acidosis, a maximum tubular capacity for bicarbonate reabsorption about half normal, growth and mental retardation, nystagmus, cataract, corneal opacities,

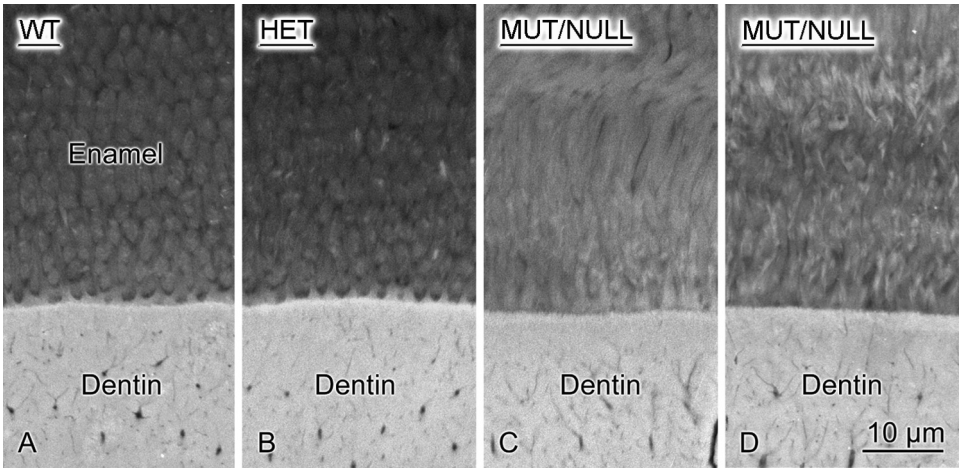

FIGURE 9. **High magnification backscattered SEM images of NBCe1 mutant animals.** Higher magnification backscattered SEM images of NBCe1$^{+/+}$ (*A*), NBCe1$^{+/-}$ (*B*), and NBCe1$^{-/-}$ (*C* and *D*) incisor enamel. *A*, *B*, and *C* are from younger enamel, and *D* is imaged from a more incisal (older enamel) position. Enamel rods are less apparent in mutant mice (*C*) when compared with normal enamel (*A* and *B*) and also apparent is the altered enamel architecture as mineralization progresses (*D*). *Scale bar* seen in *D* applies to all *panels*.

TABLE 1

Enamel and dentin microhardness

The enamel hardness of NBCe1$^{-/-}$ animals was too soft to measure. The dentin of NBCe1$^{-/-}$ animals was significantly softer than that of NBCe1$^{+/+}$ and NBCe1$^{+/-}$ animals as determined by analysis of variance ($p < 0.05$). Neither enamel nor dentin hardness differed between NBCe1$^{+/-}$ and NBCe1$^{+/+}$ animals as determined by analysis of variance or multiple comparison testing ($p > 0.05$). Values are means ± S.D. ANOVA, analysis of variance; GPa, gigapascals.

	Enamel hardness	Dentin hardness
	GPa	*GPa*
NBCe1$^{+/+}$	2.4 ± 0.2	0.37 ± 0.02
NBCe1$^{+/-}$	2.1 ± 0.1	0.35 ± 0.01
NBCe1$^{-/-}$	Too soft to measure	0.29 ± 0.02
ANOVA *p* value	$p > 0.05$	$p < 0.05$

glaucoma, and defects in the enamel consistent with amelogenesis imperfecta of permanent teeth (23). Koppang *et al.* (24) described dental and enamel abnormalities in a patient with congenital persistent proximal renal tubular acidosis (pRTA) that included agenesis of second premolars, delayed eruption of permanent teeth, and delayed shedding of the primary dentition, and severe hypoplasia. Elizabeth *et al.* (25) reported two cases of patients with renal disease that also had characteristic features of amelogenesis imperfecta. A genetic explanation of this association between renal disease and enamel malformations only recently has been established. Patients with *SLC4A4* mutations encoding NBCe1 have enamel abnormalities (7, 8), and a similar phenotype with multiorgan disease also is apparent in mice lacking NBCe1 (6). Therefore, although there are some case reports supporting a connection between pRTA and dental disease in a human population, the number of reports is limited, and because of this, the genetic and biochemical basis has not been forthcoming until recently (5).

In this study, we have focused on the dental phenotype in animals with a targeted disruption to the *Slc4a4* gene locus resulting in no NBCe1 protein expression (6). *Slc4a4* encodes for the protein NBCe1 that has three variants differing in their N and C termini. Our previous data identified NBCe1 as being expressed during enamel formation, and further, our data suggest that the NBCe1-B is the unique variant in ameloblast cells *in vivo* (Fig. 1) (5). In the model presented by Paine *et al.* (5), it was shown that the expression of NBCe1 was restricted to the basolateral membrane of ameloblasts, suggesting that this membrane protein plays an important role in regulating pH during amelogenesis. Our results demonstrate that the enamel of NBCe1$^{-/-}$ animals is abnormal, as it is hypoplastic, extremely hypomineralized, and weak. Western blotting did not reveal any significant difference in amelogenin expression among the various groups (Fig. 5). The phenotype observed on NBCe1$^{-/-}$ animals is similar to that previously described as "amelogenesis imperfecta."

Maintenance of a near physiological pH is thus important critically for normal enamel formation during the secretory and maturation stages because of the large production of hydrogen ions generated during hydroxyapatite formation (2, 26). Here, disrupting NBCe1 activity in ameloblasts, as seen in the NBCe1$^{-/-}$ animals, results in an extremely hypomineralized and weak enamel with clearly visible alterations to the expected prismatic architecture. The role of NBCe1 in amelogenesis is to allow for the passage of extracellular bicarbonate into the ameloblast cell cytoplasm from the basal or basolateral membrane, being up-regulated during the later phases of enamel formation (5). Bicarbonate is, in turn, secreted across the apical membrane via the anion exchanger AE2 (5). As pointed out however, the sequence of events regulating pH homeostasis and bicarbonate transport during amelogenesis still are being defined (5). Whereas it generally has been considered that bicarbonate act as a pH buffering mechanism in response to the release of hydrogen ion during crystal nucleation (2, 26), it may be the case that bicarbonate ions are instead transported by ameloblasts prior to the early phases of crystal nucleation (9). In this scenario, ameloblasts specifically regulate the magnitude of bicarbonate secretion as a primary event (independent of changes in extracellular pH) promoting crystal nucleation by creating a microenvironment that decreases the solubility of calcium phosphate, a crystal growth inhibitor.

In addition to having this capacity for trans-cellular bicarbonate transport, ameloblasts have the capacity to generate intracellular bicarbonate efficiently during the secretory as well as in the rough-ended stage of maturation when the cells are tightly bound and intracellular movement of ions is impeded (9, 26). In rodents, carbonic anhydrases have been identified in enamel-producing cells (ameloblasts) (11, 27–29), and a number of reports demonstrated that Car2 (carbonic anhydrase II) (27, 28) and Car6 (carbonic anhydrase VI) (29) are expressed more highly by maturation stage ameloblasts. No doubt that similar carbonic anhydrase expression profiles are evident in higher mammals. Thus, carbonic anhydrases, as well as NBCe1 and AE2, Cftr are part of the known pH regulation pathways

used by ameloblasts to maintain pH homeostasis (9), although further details of their spatiotemporal localization are yet to be fully resolved. With respect to Cftr expression in ameloblasts, it has been shown recently that Cftr localizes to the apical or secretory pole of polarized ameloblasts and is clearly up-regulated in later stages of amelogenesis (30).

NBCe1 immunoreactivity in odontoblasts suggests that NBCe1 also is expressed during dentin formation (Fig. 4, *G* and *H*). This appears confirmed by dentin hardness testing, which shows significantly softer dentin in NBCe1$^{-/-}$ animals (Table 1), although in the backscattered images of the dentin in NBCe1$^{-/-}$ animals, this is not so clearly discerned. Dentin hardness is much less affected than enamel.

In summary, NBCe1 plays an essential role in normal tooth formation during development. The biophysical properties of enamel are highly perturbed as a direct consequence of abnormal development due to the loss of NBCe1 function. Thus, although it is widely appreciated that the acidity of ingested foods, drinks, or acidic salivary pH can affect enamel once fully formed teeth are exposed to these factors in the oral cavity, the results of this study demonstrate the importance of "internal" acid-base homeostasis in the normal development of enamel in mammals.

Acknowledgments—We thank Malcolm L. Snead (University of Southern California) and Charles E. Smith (Université de Montreal and McGill University) for valuable discussions on this topic and support of this project. We thank Dr. Gary E. Shull (Department of Molecular Genetics, Biochemistry and Microbiology, University of Cincinnati College of Medicine, Cincinnati, Ohio) for breeding pairs of the NBCe1$^{+/-}$ animals and Alicia Thompson from the Scanning Electron Microscope and Analysis Center at University of Southern California. We thank Ryan Park, Archana Tank, and Grant Dagliyan of University of Southern California Molecular Imaging Center for assistance in the collection of the micro-CT data.

REFERENCES

1. Nanci, A. (2008) *Ten Cate's Oral Histology Development, Structure and Function*, 7th Ed., p. 147, Mosby Elsevier, St Louis, Missouri
2. Simmer, J. P., and Fincham, A. G. (1995) *Crit. Rev. Oral Biol. Med.* **6,** 84–108
3. Pushkin, A., and Kurtz, I. (2006) *Am. J. Physiol. Renal Physiol.* **290,** F580–599
4. Lyaruu, D. M., Bronckers, A. L., Mulder, L., Mardones, P., Medina, J. F., Kellokumpu, S., Oude Elferink, R. P., and Everts, V. (2008) *Matrix Biol.* **27,** 119–127
5. Paine, M. L., Snead, M. L., Wang, H. J., Abuladze, N., Pushkin, A., Liu, W., Kao, L. Y., Wall, S. M., Kim, Y. H., and Kurtz, I. (2008) *J. Dent. Res.* **87,** 391–395
6. Gawenis, L. R., Bradford, E. M., Prasad, V., Lorenz, J. N., Simpson, J. E., Clarke, L. L., Woo, A. L., Grisham, C., Sanford, L. P., Doetschman, T., Miller, M. L., and Shull, G. E. (2007) *J. Biol. Chem.* **282,** 9042–9052
7. Dinour, D., Chang, M. H., Satoh, J., Smith, B. L., Angle, N., Knecht, A., Serban, I., Holtzman, E. J., and Romero, M. F. (2004) *J. Biol. Chem.* **279,** 52238–52246
8. Inatomi, J., Horita, S., Braverman, N., Sekine, T., Yamada, H., Suzuki, Y., Kawahara, K., Moriyama, N., Kudo, A., Kawakami, H., Shimadzu, M., Endou, H., Fujita, T., Seki, G., and Igarashi, T. (2004) *Pflugers Arch.* **448,** 438–444
9. Lacruz, R. S., Nanci, A., Kurtz, I., Wright, J. T., and Paine, M. L. (2010) *Calcif. Tissue Int.* **86,** 91–103
10. Huang, Z., Sargeant, T. D., Hulvat, J. F., Mata, A., Bringas, P., Jr., Koh, C. Y., Stupp, S. I., and Snead, M. L. (2008) *J. Bone Miner. Res.* **23,** 1995–2006
11. Lacruz, R. S., Hilvo, M., Kurtz, I., and Paine, M. L. (2010) *Biochem. Biophys. Res. Commun.* **393,** 883–887
12. Tatishchev, S., Abuladze, N., Pushkin, A., Newman, D., Liu, W., Weeks, D., Sachs, G., and Kurtz, I. (2003) *Biochemistry* **42,** 755–765
13. Wen, X., Zou, Y., Luo, W., Goldberg, M., Moats, R., Conti, P. S., Snead, M. L., and Paine, M. L. (2008) *Anat. Rec.* **291,** 1246–1253
14. White, S. N., Paine, M. L., Sarikaya, M., Fong, H., Yu, Z., Li, Z. C., and Snead, M. L. (2000) *J. Am. Ceram. Soc.* **83,** 238–240
15. White, S. N., Miklus, V. G., Chang, P. P., Caputo, A. A., Fong, H., Sarikaya, M., Luo, W., Paine, M. L., and Snead, M. L. (2005) *J. Prosthet. Dent.* **94,** 330–335
16. White, S. N., Luo, W., Paine, M. L., Fong, H., Sarikaya, M., and Snead, M. L. (2001) *J. Dent. Res.* **80,** 321–326
17. White, S. N., Paine, M. L., Ngan, A. Y., Miklus, V. G., Luo, W., Wang, H., and Snead, M. L. (2007) *J. Biol. Chem.* **282,** 5340–5345
18. Brandes, A., Oehlke, O., Schümann, A., Heidrich, S., Thévenod, F., and Roussa, E. (2007) *Am. J. Physiol. Regul. Integr. Comp. Physiol.* **293,** R2400–2411
19. Bevensee, M. O., Schmitt, B. M., Choi, I., Romero, M. F., and Boron, W. F. (2000) *Am. J. Physiol. Cell Physiol.* **278,** C1200–1211
20. Sui, W., Boyd, C., and Wright, J. T. (2003) *J. Dent. Res.* **82,** 388–392
21. Paine, M. L., White, S. N., Luo, W., Fong, H., Sarikaya, M., and Snead, M. L. (2001) *Matrix Biol.* **20,** 273–292
22. Atkinson, M. E. (1972) *J. Periodontal Res.* **7,** 255–260
23. Winsnes, A., Monn, E., Stokke, O., and Feyling, T. (1979) *Acta Paediatr. Scand.* **68,** 861–868
24. Koppang, H. S., Stene, T., Solheim, T., Larheim, T. A., Winsnes, A., Monn, E., and Stokke, O. (1984) *Scand. J. Dent. Res.* **92,** 489–495
25. Elizabeth, J., Lakshmi Priya, E., Umadevi, K. M., and Ranganathan, K. (2007) *J. Oral Pathol. Med.* **36,** 625–628
26. Smith, C. E. (1998) *Crit. Rev. Oral Biol. Med.* **9,** 128–161
27. Toyosawa, S., Ogawa, Y., Inagaki, T., and Ijuhin, N. (1996) *Cell Tissue Res.* **285,** 217–225
28. Lin, H. M., Nakamura, H., Noda, T., and Ozawa, H. (1994) *Calcif. Tissue Int.* **55,** 38–45
29. Smith, C. E., Nanci, A., and Moffatt, P. (2006) *Eur. J. Oral Sci.* **114,** 147–153
30. Bronckers, A., Kalogeraki, L., Jorna, H. J., Wilke, M., Bervoets, T. J., Lyaruu, D. M., Zandieh-Doulabi, B., Denbesten, P., and de Jonge, H. (2010) *Bone* **46,** 1188–1196